Radiative properties of clouds over a tropical Bolivian glacier: seasonal variations and relationship with regional atmospheric circulation

Jean Emmanuel Sicart[1], Jhan Carlo Espinoza[2], Louis Quéno[1] and Melissa Medina[2]

1 IRD/UJF-Grenoble 1/CNRS/G-INP, LTHE UMR 5564, Grenoble, France

2 Instituto Geofísico del Perú (IGP). Calle Badajoz 169, Mayorazgo IV Etapa Ate. Lima-Peru

Measurements of shortwave ($S\downarrow$) and longwave ($L\downarrow$) radiation fluxes reaching Zongo glacier were analyzed from 2005 to 2013 to investigate cloud radiative properties.

A bulk cloud transmissivity for shortwave radiation ($T_n \leq 1$) was calculated at a daily time scale as:

$$S\downarrow = T_n S_{clear} = T_n T_{clear} S_{extra}$$

where S_{clear} is the shortwave clear-sky irradiance, S_{extra} is the theoretical shortwave irradiance at the top of the atmosphere and T_{clear} = 0.87 is the calibrated bulk clear-sky transmissivity.

$$L\downarrow = \varepsilon_{clear} F \sigma T^4$$

where $\varepsilon_{clear} = C (e / T)^{1/m}$ is the apparent clear sky emissivity and **$F \geq 1$ is the cloud emission factor** describing the increase in sky emissivity due to cloud emission.

The cloud cover index defined as $CI = F - T_n$ will be large for warm low clouds with high longwave emissivity and/or for thick clouds, which strongly attenuate shortwave radiation. Days with 'thick' cloud covers were identified by using the 90th percentile of CI for each season over the eight years of study, which resulted in thresholds of **CI > 0.75 for JJA, CI > 1.10 for SON and CI > 1.16 for DJF**.

The net effect of clouds on the radiation fluxes was quantified by defining **the cloud radiative forcing (CF)** as the difference between all sky and clear sky down-welling fluxes:

$$CF = S\downarrow - S_{clear} + L\downarrow - L_{clear} = S_{clear}(T_n - 1) + L_{clear}(F - 1)$$

where (T_n-1) is **negative** whereas (F-1) is **positive**.

The regional atmospheric circulation during thick cloud conditions over Zongo glacier was analyzed for the 2005-2013 period using daily **850, 500 and 200 hPa wind and geopotential height anomalies from ERA-interim reanalysis** at 0.75˚x0.75˚ horizontal resolution. We also analyzed anomalies in daily interpolated **Outgoing Longwave Radiation (OLR)** data from NCAR/NOAA at 2.5˚x2.5˚ horizontal resolution. Composite analysis of atmospheric circulation was conducted considering the beginning of intense cloudy-sky events, defined as the first day (D0) when the cloud cover index CI over Zongo was higher than the 90th percentile of all the years during the period 2005-2013. Finally, 850 hPa meridional wind anomalies were computed in the 15˚S to 25˚S and 65˚W to 57˚W region. **Days characterized by low-level incursions of southern winds to the east of the Andes were identified by positive anomalies of meridional wind in this region.**

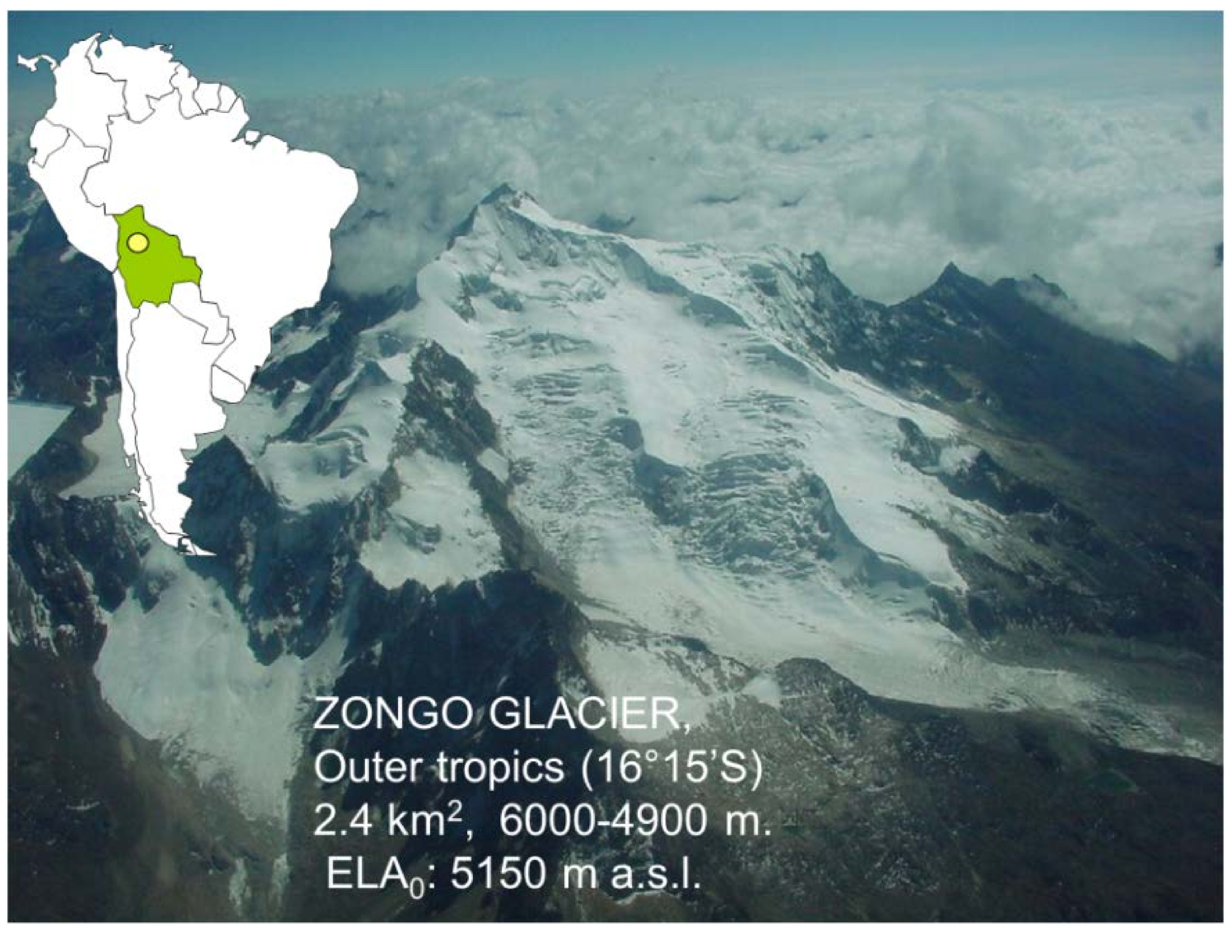

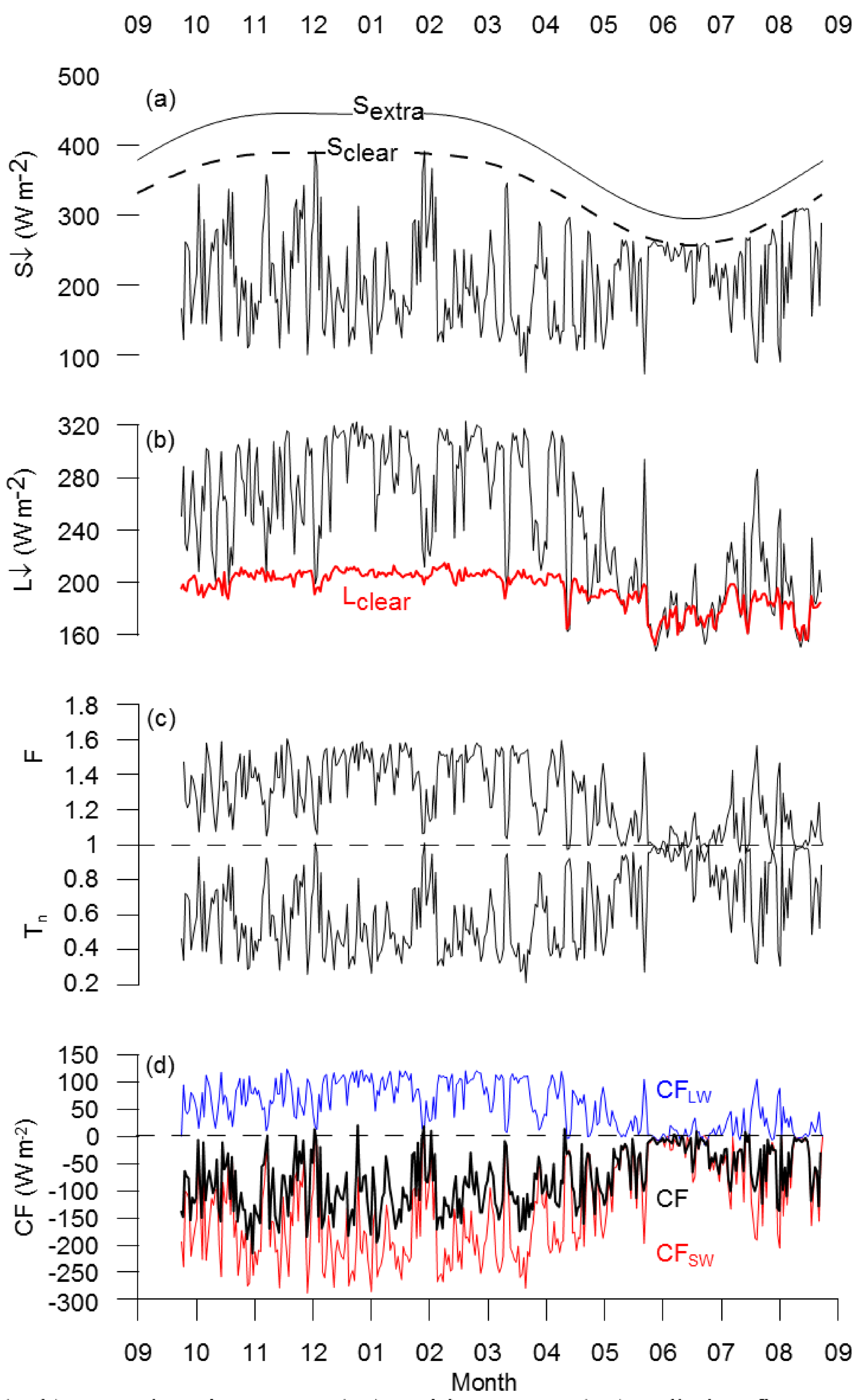

Figure 1: (a, b) Incoming short-wave ($S\downarrow$) and long-wave ($L\downarrow$) radiation fluxes, respectively. The solid and dashed line show theoretical extraterrestrial (S_{extra}) and clear-sky (S_{clear}) solar irradiance, respectively. The red line shows theoretical clear-sky long-wave irradiance (L_{clear}). (c) Cloud emission (F) and transmissivity (T_n) factors. (d) Shortwave (CF_{SW}), longwave (CF_{LW}) and all-wave (CF) cloud radiative forcing. Figures 1a-1d show daily measurements on Zongo glacier from September 2008 to August 2009.

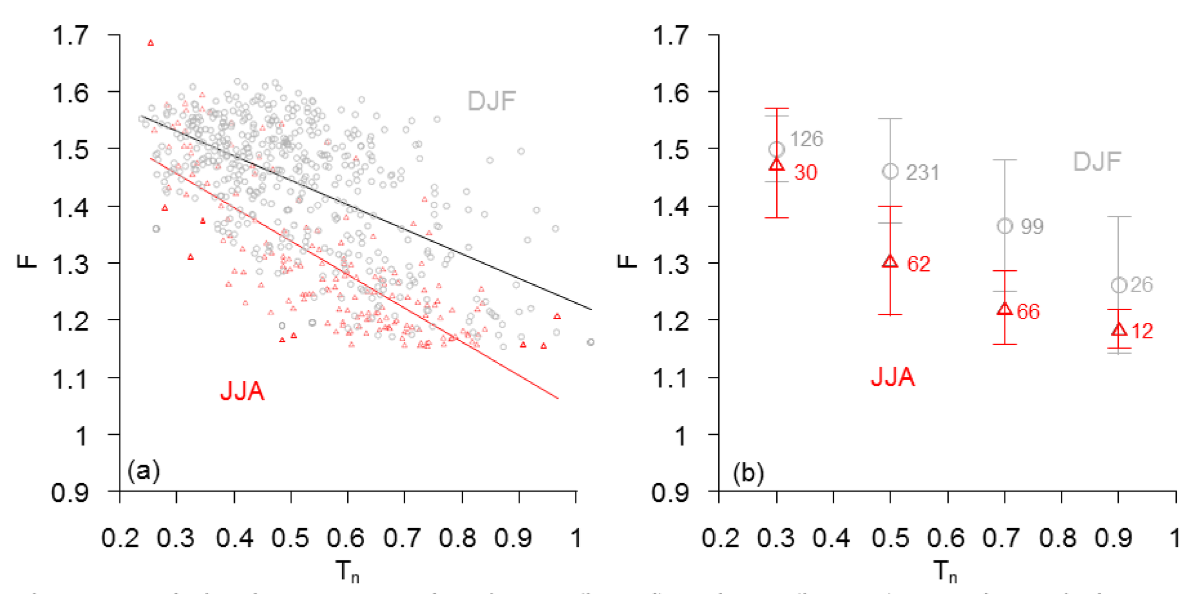

Figure 4: Relation between F and Tn in JJA (in red) and DJF (in gray) over the period 2005-2013. (a) Daily values of F according to Tn for cloudy days. Linear least-squares fit is in red in JJA (r = -0.77, n = 170) and in gray in DJF (r = -0.59, n = 482). (b) Daily values of F averaged in Tn bins (bin size = 0.2). The error bars are one standard deviation for each bin. The number at the right of data marker is the number of individual values used to create the average. JJA: June, July, August. DJF: December, January, February.

Significant seasonal changes in cloud properties were identified: shortwave radiation attenuation and longwave emission were generally greater in the wet summer season than in the dry winter season. In addition, at similar solar attenuation, clouds enhanced more longwave radiation during the wet season than during the dry season. This is probably because in the wet season clouds are frequently low warm cumulus or cumulonimbus associated with local convection, whereas the infrequent clouds in the dry season are mostly altostratus or cirrostratus associated with extra-tropical perturbations.

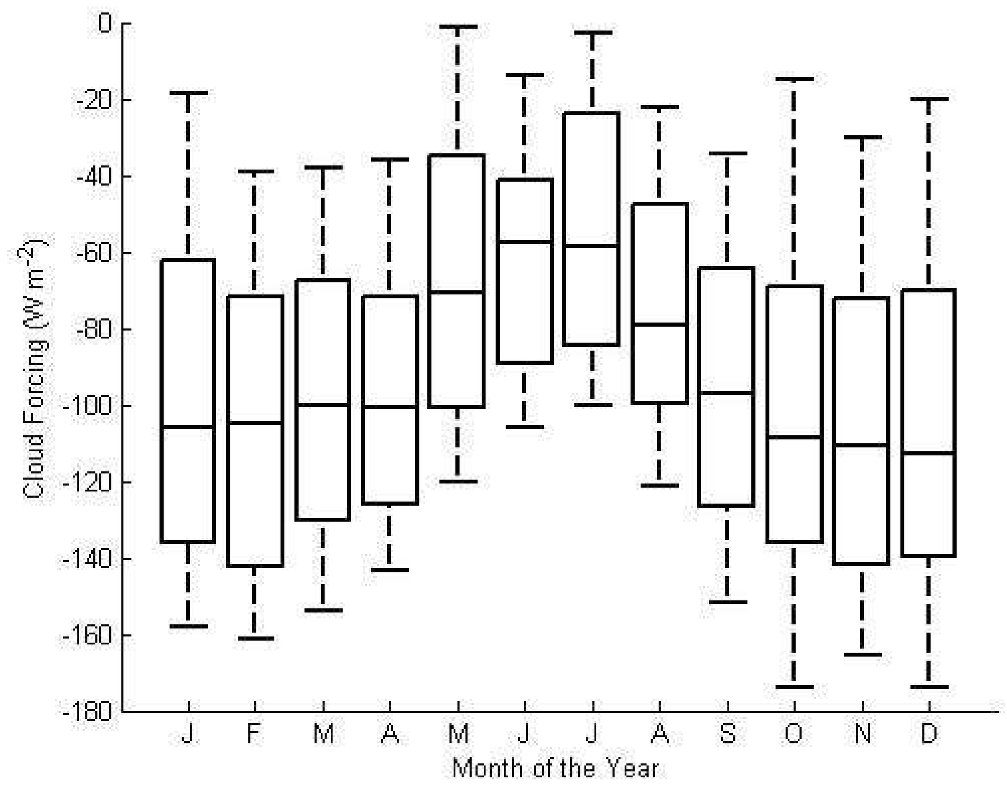

Figure 5: Monthly cloud radiative forcing CF statistics for cloudy days (F > 1.15) from 2005-2013. Box-and-whisker plots contain information on the 9th and 91st percentiles (ends of whiskers), 25th and 75th percentiles (ends of box), and median (line inside box). Numbers of cloudy days ranged from n=32 in June to n=160 in January.

Cloud radiative forcing, which results from the properties of the incident fluxes and of the clouds, was mostly negative throughout the year; with monthly averages ranging from -60 to -110 W m-2 from the dry to the wet season. Reduction in solar radiation by clouds exceeded their increase in longwave radiation largely because at low latitudes, solar irradiance is high all year long. Reduction of the down-welling fluxes due to clouds was maximal in the wet season (reaching values as low as -180 W m-2) due to high extraterrestrial solar irradiance and low shortwave transmissivity, and despite high longwave emissivity of convective clouds.

Table 1: Number of days in June, July, August (JJA) and September, October, November (SON) studied during the period 2005-2013. Frequency of days related to the beginning of severe cloudy-sky events over Zongo glacier (D0) and frequency of D0 related to low-level southern wind incursion.

	Number of days 2005-2013	Number of D0 (percent of total)	Days related to southern winds (percent of D0)
JJA	736	39 (5%)	34 (87%)
SON	729	46 (6%)	37 (80%)
DJF	722	54 (7.5%)	25(46%)

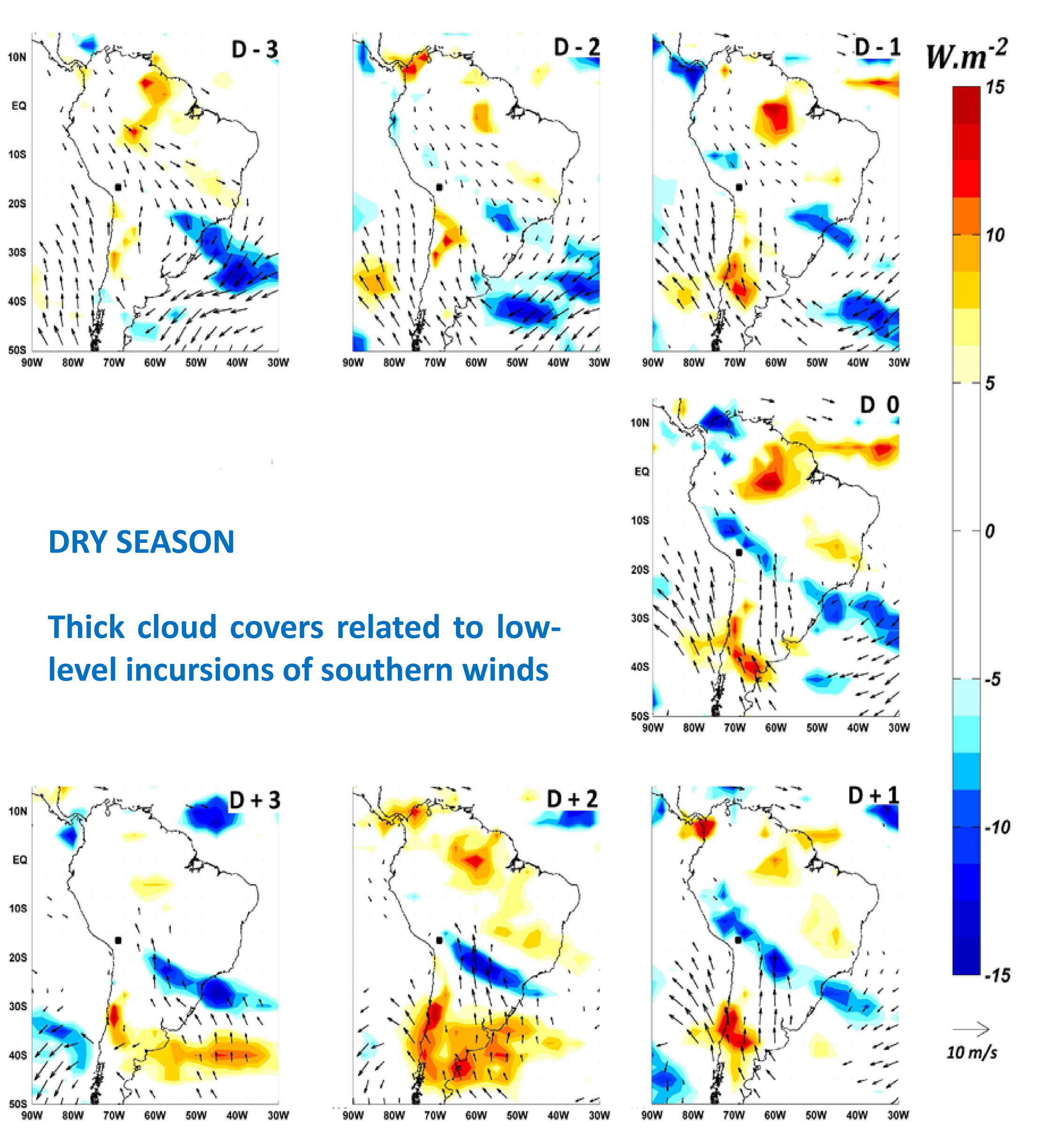

Figure 6: Composites of 850 hPa wind anomalies (vectors, m s-1) and OLR anomalies (colours, W m-2) from D–3 to D+3 from June to August (JJA) in the period 2005-2013 when thick cloud covers (CI > 0.75) over Zongo glacier were related to low-level incursions of southern wind. Only wind anomalies higher than one standard deviation are plotted. Negative [positive] OLR anomalies indicate enhanced [suppressed] convection.

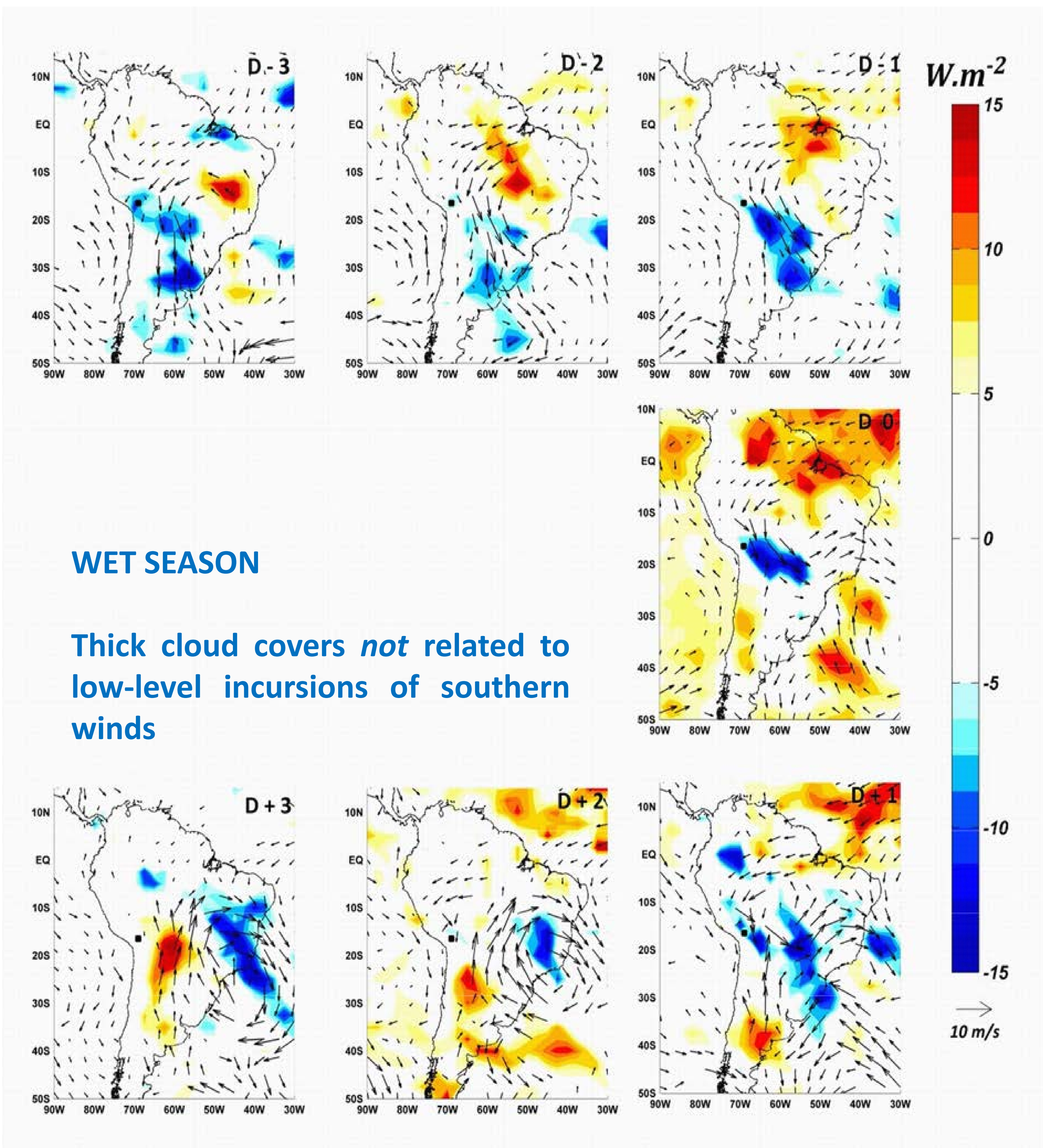

Figure 10: 2005-2013 December to February (DJF) composites of 850 hPa wind anomalies (vectors, m s-1) and OLR anomalies (colours, W m-2) from D–3 to D+3 when thick cloud covers (CI > 1.16) in Zongo are not related to low-level southern wind incursions. Only wind anomalies higher than a standard deviation are plotted. Negative [positive] OLR anomalies indicate enhanced [suppressed] convection.

In JJA and SON, clouds mostly occurred during southern wind incursions at low levels (80-87% of cases), characterizing the beginning of a cold surge episode, which generally lasts 2-3 days in the Oriental Altiplano. Other episodes of cloud cover in the dry season (JJA) were linked to low pressure conditions at 200 hPa on the Chilean coast (including cut-off low episodes), whereas in SON, they were linked to early summer conditions characterized by an active Bolivian High and easterly winds at 200 hPa over the Cordillera Real. During the wet season, thick cloud covers were still often associated with southern wind incursions (46% of cases), other cloud events being associated with the South American Monsoon, intensification of the Bolivian High and enhancement of the easterly winds at 200 hPa over the Altiplano. Composite analysis during the wet season suggests that large cloud conditions in the Bolivian Oriental Andes mainly occur during the transition from SESA to SACZ dipole-like pattern.

IRD GLACIOCLIM GREATICE LTHE